Radiat Environ Biophys (2003) 42:201–211
DOI 10.1007/s00411-003-0206-7

ORIGINAL PAPER

Paweł Możejko · Léon Sanche

Cross section calculations for electron scattering from DNA and RNA bases

Received: 17 February 2003 / Accepted: 30 July 2003 / Published online: 11 September 2003

Abstract Differential and integral cross sections for elastic electron collisions with uracil, cytosine, guanine, adenine and thymine have been calculated using the independent atom method with a static-polarization model potential for incident energies ranging from 50 to 4000 eV. Total cross sections for single electron-impact ionization of selected DNA and RNA bases have also been calculated with the binary-encounter-Bethe model from the ionization threshold up to 5000 eV. Cross sections within the investigated energy range, can be related to the molecular symmetry, the number of target electrons and molecular size; elastic and ionization processes are most efficient for guanine and adenine molecules, while the lowest cross sections were obtained for the uracil molecule. The ionization cross sections for cytosine, thymine, adenine and guanine are compared with those recently obtained with a semi-classical and binary-encounter-Bethe formalisms. No theoretical and experimental data for elastic electron scattering from DNA and RNA bases are available, but comparisons with calculations for molecules of similar size and geometry allows the validity of the theoretical approach to be verified.

Introduction

Uracil ($C_4H_4N_2O_2$), thymine ($C_5H_6N_2O_2$) and cytosine ($C_4H_5N_3O$), as well as adenine ($C_5H_5N_5$) and guanine ($C_5H_5N_5O$) molecules are some of the simplest pyrimidine and purine bases, respectively, and are components of deoxyribonucleic (DNA) and ribonucleic (RNA) acids. These nucleic acids whose function is the storage and transfer of genetic information [1], are essential components of all living cells.

The interaction of ionizing radiation (i.e. β-rays, x-rays, or γ-rays) with living cells induces different types of damage in DNA and RNA such as single-strand breaks, double-strand breaks, base deletions etc. [2, 3, 4]. Such modifications of cellular DNA and RNA promote cytotoxic, mutagenic and carcinogenic lesions and are the result of energy transfers that occur via a variety of excitation and ionization processes producing large quantities of radicals, ions and secondary electrons [4, 5, 6, 7, 8, 9].

The process of DNA damage induced along ionization radiation tracks is usually modeled with Monte Carlo simulations [4, 5, 6, 7, 8, 9, 10] for which a complete set of cross sections for the interaction of the primary and secondary fast particles with target molecules is needed. Usually, in these simulations a simplified linear segment of DNA or structured higher ordered DNA target (e.g. a nucleosome core particle or a piece of chromatin fiber [10]) occupies a given volume within the irradiated medium, e.g., in the form of a cylinder [8]. Using liquid water as the irradiated medium containing DNA, a Monte Carlo track structure simulation code (e.g. CPA100 [11], OREC [12], PARTRAC [13, 14]) provides the history of electron interactions in the solvent with that portion of the energy which is deposited in the DNA. From this information the damage induced in the DNA can be evaluated [6]. The input data sets for such simulations include mainly cross sections for primary and secondary electron interactions with liquid and/or gaseous water (e.g. [9]).

It has been demonstrated that not only high-energy projectiles but also electrons of lower energies can induce DNA damage [3, 15, 16, 17, 18, 19, 20]. Electrons with energies below 15 eV, which are produced in large quantities by ionizing radiation (~4×10^4 per MeV [21, 22]), can induce single-strand and double-strand breaks in DNA [15, 16] via electron resonances (i.e. the formation of transient anions) [19, 23, 24, 25, 26, 27] with a substantial cross section [16]. Similar cross sections are found at higher energies [16]. Hence it appears that in order to refine theoretical modeling of radiation damage

P. Możejko (✉) · L. Sanche
Groupe des Instituts de Recherche en Santé du Canada en Sciences des Radiations, Faculté de Médecine,
Université de Sherbrooke,
3001 12 Avenue Nord, Sherbrooke , Québec, J1H 5N4, Canada
e-mail: Pawel.Mozejko@Usherbrooke.ca
Tel.: +1-819-5645403
Fax: +1-819-5645442

to cellular DNA and RNA, more input data on the action of electrons on DNA are needed, particularly on the interaction of secondary electrons of low energy with the basic components of these acids (e.g., the bases).

In this paper, we report elastic and ionization cross section calculations for 50–3000 eV electron scattering from DNA and RNA bases. These two processes dominate the scattering of electrons from atoms and molecules in this energy range. In elastic collisions, the impinging electron, e^-, does not change its kinetic energy, E_i, and a scattering molecule remains at the same energetic state:

$$(AB)_i + e^-(E_i) \rightarrow (AB)_i + e^-(E_i)$$

where i denotes initial energetic state of a hypothetical diatomic molecule AB.

In the electron-impact ionization process in which a positive ion AB^+ is produced, the scattered electron $e^-(E_i)$ loses part of its initial kinetic energy and an additional electron, $e^-(E_i - E_{\text{ion}} - E_f)$ is ejected from molecule AB:

$$(AB)_i + e^-(E_i) \rightarrow (AB)_f^+ + e^-\left(E_f\right) + e^-\left(E_i - E_{\text{ion}} - E_f\right)$$

where E_{ion} and E_f are the binding energy of the electron within the AB molecule and final energy of the primary electron, respectively. While elastic scattering dominates in electron collisions with atoms and molecules, above 70 eV electron impact ionization is the most efficient inelastic process.

Since low energy electron (LEE) interaction with DNA and RNA is a complex process, there is a need to develop a relatively simple theoretical approach to calculate LEE scattering cross sections from these molecules. As a starting point, such a simple approach can be tested on basic components of DNA and later be extended to include larger portions of the DNA molecule. Since cross sections are also presently being generated experimentally for the DNA bases [28], it should become possible to check in which energy range the present simplified theoretical approach, namely the independent particle model can be employed in calculations.

To our knowledge this is the first attempt to generate elastic cross sections for DNA and RNA bases within the intermediate energy range (50–4000 eV). Very recently, electron impact ionization cross sections for constituents of DNA, namely cytosine, thymine, adenine, guanine and the sugar-phosphate backbone, over the energy range from the ionization threshold to 1000 eV have been obtained with the Deutsch-Mark semi-classical formalism and the binary-encounter-Bethe method by Bernhardt and Paretzke [29]. Ionization and fragmentation of the uracil molecule by electron impact have been studied experimentally by Coupier et al. [30]. In the two following sections we describe the theoretical approaches and give the results.

Theory and computational methods

In the present work, we employed two relatively simple calculation methods to generate these cross sections: differential (DCS) as well as integral cross sections (ICS) for elastic electron scattering have been obtained with the independent atom method, while electron-impact ionization cross sections has been calculated with the binary-encounter-Bethe method.

Independent atom method

In this subsection, for convenience, we adopted atomic units in which $e=m_e=\hbar=1$, but the final results of calculations are given in the SI units.

Calculations of elastic cross sections have been carried out using the independent-atom method (IAM) [31, 32, 33] with a static-polarization model potential. In this approximation, an electron-molecule collision is reduced to the problem of collision with individual atoms: it is assumed that each atom of the molecule scatters independently, any redistribution of atomic electrons due to the molecular binding is unimportant, and multiple scattering within the molecule is negligible [31]. This approach offers reasonable approximations to elastic, momentum transfer and total cross sections for intermediate energy and high energy electrons and/or positron scattering from many polyatomic molecular targets [32, 33, 34, 35, 36, 37, 38, 39, 40, 41, 42, 43, 44, 45].

In the simple form of the independent atom approximation, the DCS for elastic electron scattering on molecules, taking into account all possible orientations of the intermolecular axis in the space, is given by:

$$\frac{d\sigma}{d\Omega} = \sum_{j=1}^{N} \frac{d\sigma^A}{d\Omega_j} + \sum_{i\neq j=1}^{N} f_i(\theta,k) f_j^*(\theta,k) \frac{\sin\left(sr_{ij}\right)}{sr_{ij}} \tag{1}$$

where N is the number of atoms within molecule, θ the scattering angle, $\frac{d\sigma^A}{d\Omega_j}$ the elastic differential cross section of the j-th atom, and $f_i(\theta,k)$ and $f_j^*(\theta,k)$ the complex scattering amplitudes due to the i-th and j-th atom of the molecule, respectively. In Eq. 1, k denotes the incident electron wave number and $s=2k\sin(\theta/2)$ the magnitude of the momentum transfer during the collision. The internuclear distance between the i-th and j-th atom of the target molecule is represented by r_{ij}. The internuclear distances r_{ij} for guanine, adenine, thymine, cytosine and uracil were obtained using a geometry optimization procedure with the *ab initio* quantum chemistry package GAMESS (General Atomic Molecular Electronic Structure System) [46] with a built in "triple-split" Gaussian basis set (6-311G) [47] and by choosing the framework symmetry group as C_1. Geometrically optimized structures of the investigated molecules are very close to those published previously [48, 49], with discrepancies in bond lengths and bond angles less than 0.01 Å and 1°, respectively. The small discrepancies are mainly due to different basis sets and methods used in optimization procedures.

It follows from the optical theorem that the ICS for electron elastic scattering on the molecule in the IAM approximation is given by:

$$\sigma(E) = \frac{4\pi}{k}\text{Im}\, f(s=0,k) = \frac{4\pi}{k}\sum_{i=1}^{N}\text{Im}\, f_i(\theta=0,k) = \sum_{i=1}^{N}\sigma_i(E) \tag{2}$$

where $\sigma_i(E)$ is the ICS of the i-th atom of the molecule at energy $E=k^2/2$.

To obtain the atomic scattering amplitudes and elastic electron-atom cross sections, we employed partial wave analysis [50] and solved numerically with the Numerov method [51] (for details see Appendix A) the radial Schrödinger equation:

$$\left[\frac{d^2}{dr^2} - \frac{l(l+1)}{r^2} + k^2 - 2\left(V_{stat}(r) + V_{polar}(r)\right)\right] u_l(r) = 0 \tag{3}$$

under the boundary conditions:

$$u_l(0) = 0,\ u_l(r) \overrightarrow{r \to \infty} A_l \hat{j}_l(kr) - B_l \hat{n}_l(kr) \quad (4)$$

where $\hat{j}_l(kr)$ and $\hat{n}_l(kr)$ are the spherical Bessel-Riccati and Neumann-Riccati functions [52] (for basic definition see Appendix B), respectively. $V_{\text{stat}}(r)$ is the static potential of the atom expressed in the form proposed by Salvat et al. [53]:

$$V_{stat}(r) = -\frac{Z}{r}\sum_{n=1}^{3} a_n \exp(-\beta_n r) \quad (5)$$

where Z is the nuclear charge, and a_n and β_n are the parameters determined by an analytical fitting procedure to Dirac-Hartree-Fock-Slater self-consistent data [53]. For this formulation, it has been shown [53] that n=1,...,3 is sufficient to obtain a reliable static potential (i.e. comparable to that obtained directly from the Dirac-Hartree-Fock-Slater functions). The polarization potential $V_{\text{polar}}(r)$ was expressed in the form proposed by Padial and Norcross [54]:

$$V_{polar}(r) = \begin{cases} v(r) & r \leqslant r_c \\ -\alpha/2r^4 & r > r_c \end{cases} \quad (6)$$

where $v(r)$ is the free-electron-gas correlation energy [55] and α is the static electric dipole polarizability of an atom. The distance r_c is that of the first crossing point of the $v(r)$ and $-\alpha/2r^4$ curves [56]. In the present study, we neglected exchange effects as these have been found to be negligible at high incident energies. Furthermore, our previous work [33] has shown that the IAM method, with static and polarization potentials only, can reproduce very well experimental elastic DCS and ICS even for low (~20 eV) collision energies.

The scattering amplitudes for electron scattering on atom were obtained using the following equation:

$$f(\theta,k) = \frac{1}{2ik}\sum_{l=0}^{l_{\max}} (2l+1)\left(e^{2i\delta_l} - 1\right) P_l(\cos\theta) + \pi\alpha k\left(\frac{1}{3} - \frac{1}{2}\sin\frac{\theta}{2} - \sum_{l=1}^{l_{\max}} \frac{P_l(\cos\theta)}{(2l-1)(2l+3)}\right) \quad (7)$$

where $P_l(\cos\theta)$ are Legendre polynomials and the second term in Eq. 7 is the Born scattering amplitude (i.e. the scattering amplitude generated within the Born approximation) for a potential of the form from Eq. 6 [57]. In the present calculations, we obtained for the first $l_{\max}$=50, the exact phase shifts and the contribution of those remaining (from $l_{\max+1}$ to ∞) is included through the Born approximation. The phase shifts δ_l are connected with the asymptotic form of the wave function, $u_l(r)$, by:

$$\tan\delta_l = \frac{B_l}{A_l} \quad (8)$$

The DCS for elastic electron scattering from a particular atom, $\frac{d\sigma^A}{d\Omega}$, was calculated according to:

$$\frac{d\sigma^A}{d\Omega} = |f(\theta,k)|^2 \quad (9)$$

while the atomic elastic ICS cross section, σ^{A}, was derived from the following expression:

$$\sigma^A = \frac{4\pi}{k^2}\left(\sum_{l=0}^{l_{\max}} (2l+1)\overset{2}{\sin}\delta_l + \sum_{l=l_{\max}}^{\infty} (2l+1)\overset{2}{\sin}\delta_l^{(B)}\right) \quad (10)$$

Since the above theoretical and numerical approaches have yielded encouraging results for polyatomic molecular targets like XY_4 (X=C, Si, Ge; Y=H, F, Cl) and for C_2F_6 [33, 58], it is expected that the differential cross sections and integral cross sections for electron elastic scattering by more complex molecules, such as those presented here may also be fairly reliable.

Binary-encounter-Bethe (BEB) method

Electron-impact ionization cross sections have been calculated using the binary-encounter-Bethe model [59, 60], which is a simplified version of the binary-encounter-dipole model [59]. This method is based on a combination of two earlier theories, the Mott theory [61] and the Bethe [62, 63] theory and has been successfully employed for calculation of total electron-impact ionization cross sections of a variety of molecules of atmospheric [64] and industrial interest [65, 66]. In this approximation the electron-impact ionization cross section per molecular orbital is given by:

$$\sigma_{BEB} = \frac{S}{t+u+1}\left[\frac{\ln t}{2}\left(1 - \frac{1}{t^2}\right) + 1 - \frac{1}{t} - \frac{\ln t}{t+1}\right] \quad (11)$$

where u=U/B, t=T/B, S=$4\pi a_0^2 N R^2/B^2$, a_0=0.5292 Å, R=13.61 eV, and T is the energy of impinging electrons. Finally, the total cross section for electron-impact ionization was obtained as the sum of σ_{BEB} for all molecular orbitals.

The electron binding energy B, kinetic energy of the orbital, U, and orbital occupation number, N, were obtained for the ground states of the investigated molecules with the Hartree-Fock method using the GAMESS code [46] and the Gaussian 6-311G basis set. Because the valence orbital energies obtained in this way differ slightly from those obtained with other theories [67, 68, 69] and experimental ones [70, 71, 72], we also performed outer valence Green function calculations of correlated electron affinities and ionization potentials [73, 74, 75, 76] with the GAUSSIAN code [77]. The experimental values [70, 71] of the first ionization potential were inserted in the calculation, instead of those obtained theoretically, to fix the threshold behavior of the ionization cross section at the experimental value. In Table 1, we compare the values of the first ionization potential obtained in the different theoretical calculations and experiments. The values of B, U, and N for uracil, thymine, cytosine, adenine and guanine, incorporated in

Table 1 Selected ionization potentials[3] of DNA and RNA bases obtained from different theoretical methods and experiments

Method	Ionization potential (eV)					
	Uracil	Cytosine	Thymine	Adenine	Guanine	Reference
B3LYP/6-311++G**	9.25	8.59	8.76	8.12	7.68	[67]
B3PW91/6-311++G**	9.33	8.66	8.85	8.14	7.69	[67]
BP/6-311++G**	9.27	8.79	8.79	8.10	7.68	[67]
MP2/6-31+G*	-	8.74	8.85	8.18	7.66	[67]
B3LYP/6-311G(2df,p)	9.21	8.57	8.74	8.09	7.64	[68]
RHF/3-21G	-	9.01	9.48	8.48	8.05	[29]
RHF/6-311 G (GAMESS)	10.16	9.34	9.75	8.72	8.35	Present theory
ROVGF/6-311 G (GAUSSIAN)	8.97	8.12	8.53	8.02	7.44	Present theory
Experimental	-	8.68	8.87	8.26	7.77	[70]
Experimental	8.35±0.01	-	-	-	-	[71]
Experimental	-	-	-	8.55±0.10	-	[72]

Table 2 Molecular orbitals, electron binding energy and kinetic energy for uracil, cytosine, thymine, adenine and guanine

MO	Uracil		Cytosine		Thymine		Adenine		Guanine	
	B	U	B	U	B	U	B	U	B	U
1	559.3	794.1	558.0	794.0	559.3	794.1	425.6	601.4	558.6	794.0
2	559.3	794.1	425.4	601.5	559.1	794.1	424.1	601.7	425.6	601.4
3	426.0	601.5	424.4	601.4	425.8	601.5	424.0	601.3	425.5	601.5
4	425.6	601.5	423.2	601.6	425.5	601.5	423.8	601.6	424.9	601.4
5	311.4	435.9	310.0	435.9	311.3	435.9	423.5	601.6	423.9	601.6
6	310.4	435.9	309.5	435.9	310.3	435.9	309.1	435.8	423.8	601.7
7	308.9	435.8	308.7	435.8	308.6	435.8	308.6	435.7	310.8	435.9
8	306.7	435.7	306.5	435.6	306.9	435.7	308.5	435.7	309.0	435.9
9	39.76	61.89	38.34	61.13	306.0	435.8	308.2	435.8	308.7	435.8
10	38.76	69.71	35.88	56.41	39.64	61.64	306.8	435.6	308.0	435.8
11	36.18	59.11	34.83	54.68	38.71	69.65	37.99	47.59	306.5	435.6
12	34.41	57.75	32.40	55.07	36.01	59.36	36.13	49.59	38.67	57.80
13	30.19	47.89	29.57	47.79	34.31	57.56	34.46	52.34	37.70	55.30
14	25.82	43.50	24.94	44.77	30.65	45.68	32.79	56.05	37.03	54.12
15	24.99	52.31	24.41	48.31	26.78	41.79	31.82	56.88	33.77	52.96
16	22.42	39.72	21.26	37.51	25.38	41.68	28.90	49.55	33.64	57.37
17	21.35	44.20	21.13	40.57	24.83	50.42	24.89	46.04	32.48	56.46
18	17.47	39.71	20.03	46.17	21.43	42.88	24.30	46.23	28.77	50.67
19	16.25	35.30	16.85	41.45	21.40	43.51	23.33	45.31	25.14	45.95
20	16.20	54.61	15.20	43.14	17.30	40.10	21.70	41.29	24.69	49.02
21	15.55	55.06	15.11	33.17	16.17	34.63	20.51	42.55	23.18	45.39
22	14.56	59.57	14.65	42.36	16.14	55.42	17.23	40.27	22.44	40.13
23	14.45	45.68	13.86	60.95	15.12	60.01	16.52	47.58	20.75	43.27
24	13.85	43.18	13.06	38.13	14.88	53.86	15.60	30.26	20.52	47.56
25	12.66	40.97	11.76	41.54	14.82	30.57	15.52	44.28	17.45	43.93
26	11.12	63.08	9.56	61.60	13.63	42.69	15.13	45.43	16.56	46.47
27	10.18	65.30	9.38	54.81	13.43	40.10	14.31	42.48	15.78	31.80
28	10.05	65.30	8.91	43.66	13.47	33.43	13.60	34.70	15.26	49.35
29	8.35	49.96	8.68	45.78	12.31	41.94	12.14	35.98	14.48	44.63
30					10.98	62.66	11.02	51.76	14.34	63.78
31					10.14	64.81	10.23	42.73	14.33	35.03
32					9.97	55.67	9.98	51.48	13.23	41.05
33					8.87	41.52	9.28	39.90	10.88	51.10
34							8.99	52.12	10.63	41.58
35							8.26	39.89	9.99	48.79
36									9.80	63.50
37									9.38	54.22
38									9.71	43.57
39									7.77	41.75

the computation of electron-impact ionization cross sections are presented in Table 2.

Results and discussion

Differential and integral cross sections

Differential cross sections for elastic electron scattering from uracil, thymine, cytosine, adenine and guanine are presented in Figs. 1 and 2 for electron energies of 50 (*short dashed line*), 100 (*dotted line*), 200 (*solid line*) and 500 eV (*dotted and dashed line*). There is no elastic measurement and calculation to be compared with these results.

The angular dependence of DCS values is very similar for all investigated pyrimidine bases, which reflects the similarity in molecular structure, especially the molecular geometry of uracil, cytosine and thymine. Comparison of the angular distributions of scattered electrons for adenine and guanine also shows a large similarity in the cross sections for the purine bases related to similarity in the geometry. Although the difference in geometry of purine and pyrimidine bases is significant, the shape of the DCSs for pyrimidine bases differs only slightly from those of the purine bases. This means that the main contribution to DCS in Eq. 1 comes from terms with $i=j$, i.e. the contribution from interference terms ($i\neq j$) is rather small so that the cross section depends mainly on the molecular size and numbers of atoms. For scattering angles ranging from 3° to 180° the cross section value for each molecule studied decreases with increasing electron energy. Only for forward scattering angles (i.e. scattering within 0–3°) does the contribution to the elastic DCS increase with collision energy (see comparison in Table 3).

Generally, the calculated DCSs for elastic electron scattering from DNA and RNA bases are typical for elastic differential cross sections of other polyatomic molecules [33, 40, 42, 58]. The highest values of the elastic DCSs are obtained for the largest molecule (i.e. guanine) and the lowest for uracil which is the smallest

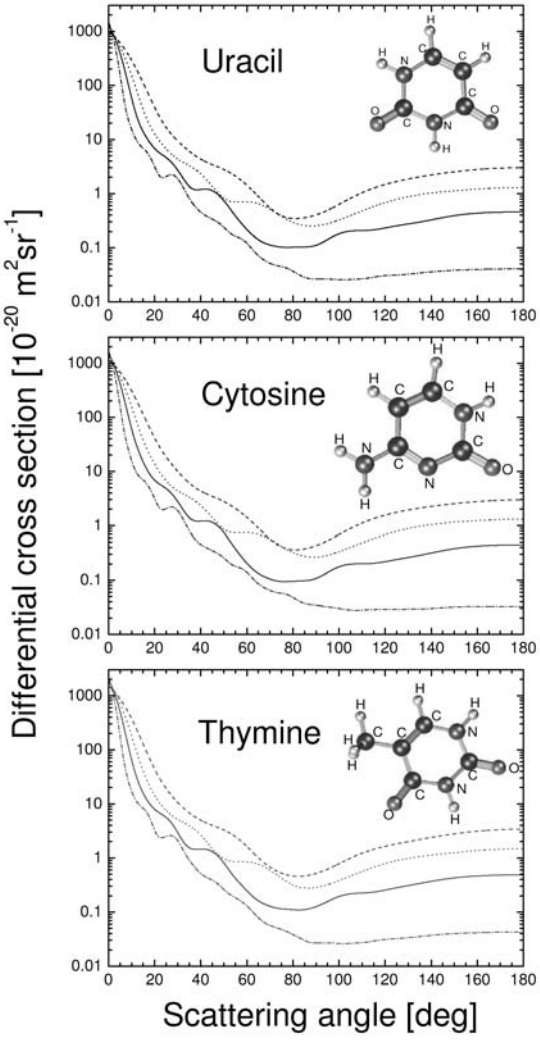

Fig. 1 Differential cross section for 50 eV (*short dashed line*), 100 eV (*dotted line*), 200 eV (*solid line*), and 500 eV (*dotted and dashed line*) elastic electron scattering from uracil, cytosine, and thymine

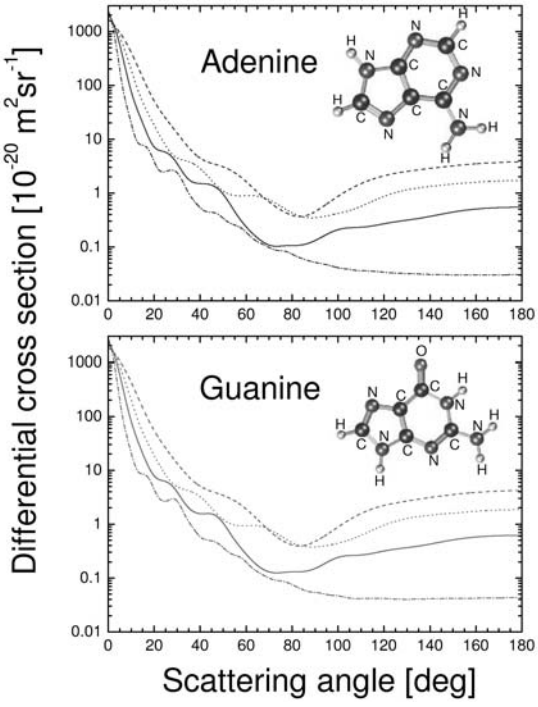

Fig. 2 Differential cross section for 50 eV (*short dashed line*), 100 eV (*dotted line*), 200 eV (*solid line*), and 500 eV (*dotted and dashed line*) elastic electron scattering from adenine and guanine

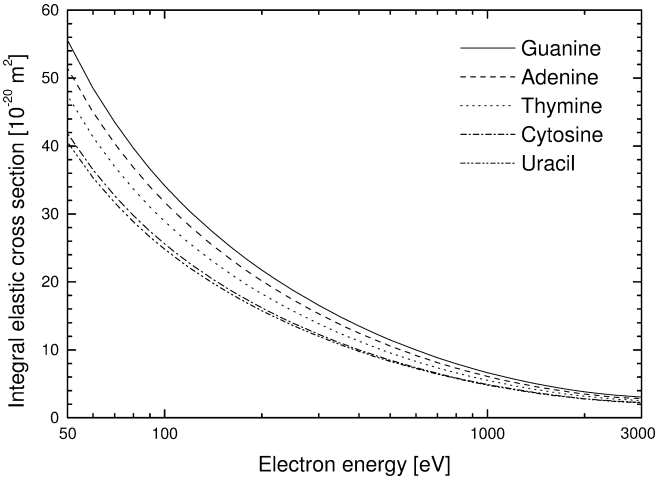

Fig. 3 Energy dependence of integral elastic cross sections for electron collisions with guanine, adenine, thymine, cytosine and uracil

investigated molecule. Thus, the elastic DCS value appears to be essentially connected with number of electrons in the molecule and molecular size, while angular dependence of the elastic DCSs is related to molecular geometry.

The incident electron energy dependence of the ICSs for the investigated molecular targets are presented in Fig. 3 and the values of the ICSs at selected energies are listed in Table 4.

In each case, the integral elastic cross sections are monotonically decreasing functions of impact energy and also dependent on molecular size. The integral elastic cross section values are highest for guanine and adenine molecules and lowest for cytosine and uracil over the entire energy range investigated.

In Fig. 4, we compared elastic ICS for the uracil molecule with cross sections obtained previously [58] for benzene (C_6H_6), hexafluorobenzene (C_6F_6), chlorobenzene (C_6H_5Cl) and fluorobenzene (C_6H_5F) with the same method. It is evident that the energy dependence of the ICS for uracil is similar to other ring molecules of similar size. Its value is higher than the cross sections values for benzene and fluorobenzene molecules and lower than the corresponding values for chlorobenzene and hexafluorobenzene. Thus, in this case ICS values strongly depend on the molecular size and on the nature of the outermost atoms.

Table 3 Differential cross sections (DCS) for elastic electron scattering in the forward direction from uracil, cytosine, thymine, adenine and guanine in units of 10^{-20} m^2 sr^{-1}

	Energy (eV)	Scattering angle (deg)					
		0	1	2	3	4	5
Uracil	50	1007	932	850	766	689	613
	100	1113	998	870	743	628	522
	200	1270	1089	889	697	534	396
	500	1450	1128	778	487	288	160
Cytosine	50	1144	1058	961	863	771	682
	100	1259	1126	977	828	693	568
	200	1438	1230	995	769	579	421
	500	1621	1252	847	515	269	162
Thymine	50	1497	1382	1252	1120	996	875
	100	1652	1474	1273	1070	887	719
	200	1871	1594	1276	971	718	509
	500	2121	1623	1072	628	346	181
Adenine	50	1665	1537	1392	1242	1102	965
	100	1840	1641	1414	1185	978	788
	200	2127	1812	1448	1097	806	568
	500	2383	1824	1201	698	382	202
Guanine	50	1861	1718	1553	1382	1220	1063
	100	2051	1829	1570	1306	1068	851
	200	2369	2015	1597	1192	860	596
	500	2678	2037	1311	739	395	207

Table 4 Cross sections for elastic electron scattering from guanine, adenine, thymine, cytosine and uracil at selected energies

Energy (eV)	Integral elastic cross section (10^{-20} m^2)				
	Guanine	Adenine	Thymine	Cytosine	Uracil
50	55.56	51.48	47.43	41.84	40.55
60	48.53	45.01	41.34	36.50	35.36
70	43.49	40.36	36.97	32.67	31.65
80	39.67	36.83	33.67	29.76	28.85
90	36.65	34.03	31.05	27.47	26.63
100	34.18	31.73	28.92	25.59	24.82
110	32.11	29.81	27.13	24.02	23.30
120	30.34	28.16	25.61	22.67	22.01
140	27.45	25.47	23.12	20.49	19.90
160	25.17	23.35	21.17	18.76	18.24
180	23.31	21.61	19.58	17.36	16.89
200	21.75	20.16	18.25	16.19	15.76
220	20.42	18.92	17.12	15.18	14.79
250	18.75	17.35	15.69	13.92	13.58
300	16.55	15.30	13.83	12.28	11.99
350	14.86	13.73	12.40	11.01	10.76
400	13.51	12.46	11.26	10.00	9.784
450	12.39	11.43	10.33	9.170	8.980
500	11.46	10.56	9.544	8.475	8.306
600	9.977	9.182	8.302	7.372	7.234
700	8.848	8.135	7.357	6.533	6.418
800	7.958	7.310	6.614	5.873	5.775
900	7.238	6.644	6.013	5.340	5.254
1000	6.644	6.095	5.518	4.900	4.824
1100	6.146	5.635	5.103	4.532	4.463
1200	5.723	5.245	4.750	4.219	4.156
1400	5.045	4.621	4.186	3.718	3.664
1600	4.530	4.148	3.758	3.339	3.290
1800	4.132	3.783	3.427	3.045	3.000
2000	3.819	3.497	3.168	2.816	2.772
2200	3.574	3.273	2.964	2.636	2.592
2500	3.303	3.028	2.742	2.440	2.394
3000	3.052	2.803	2.541	2.263	2.209
3500	2.997	2.760	2.511	2.235	2.168
4000	3.114	2.876	2.633	2.342	2.255

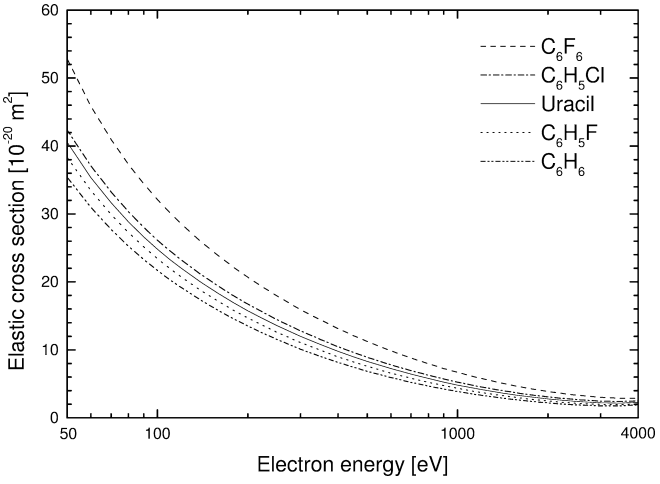

Fig. 4 Comparison of the energy dependence of integral elastic cross sections for electron scattering from hexafluorobenzene (C_6F_6), chlorobenzene (C_6H_5Cl), uracil ($C_4H_4N_2O_2$), fluorobenzene (C_6H_5F) and benzene (C_6H_6). The results for C_6F_6 and benzene were calculated by Możejko et al. [58]. The other were generated in the present investigation

It is worth noting that in mathematical form the main assumptions of the independent atom method can be expressed by $kR>>1$, where k is the momentum of the incident electron (in a.u.) and R the typical internuclear distance (in a.u.) in the target molecule. In the present study, at the lowest energies, the kR value is greater than 1 for all investigated molecules. However, below 50 eV, the approximation can give values too high for the elastic ICS. Usually, elastic cross sections obtained with IAM for electron scattering from polyatomic molecules, exceed the total (elastic + inelastic) cross section values for collision energies lower than 10 eV. Such disagreements

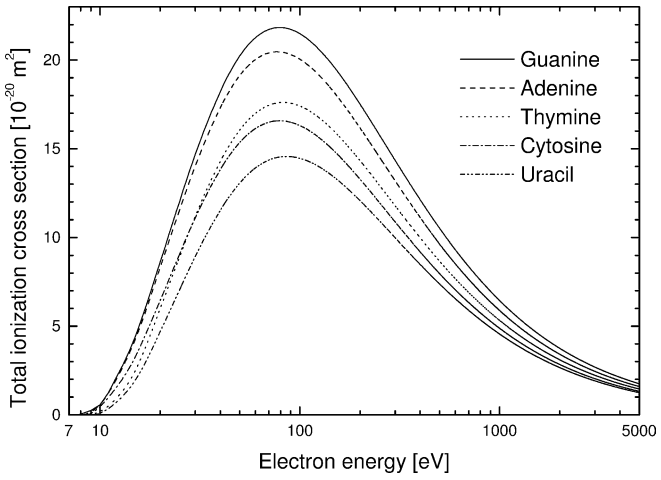

Fig. 5 Energy dependence of total cross sections for electron-impact ionization of guanine,adenine, thymine, cytosine and uracil

[33, 58] can be due to neglect of the bond distortion and multiple scattering at impact energies, corresponding to electron wavelengths comparable to internuclear distances. However, it should be noted that even at collision energies as low as 20 eV, for some small molecules (e.g., SiH_4 and GeH_4), the IAM method yields elastic ICS in very good agreement with experimental findings [33].

Total cross section for electron impact ionization

Figure 5 shows the calculated total cross sections for single electron-impact ionization of uracil, cytosine, thymine, adenine and guanine. They are listed at selected energies in numerical form in Table 5. For each molecule the cross section maximum is located near 80 eV. Ionization processes are most efficient for guanine and adenine with a cross section maximum exceeding 2×10^{-19} m^2. Ionization cross sections for thymine and cytosine are very similar especially at the threshold and uracil has the lowest ionization cross section.

Recently, ionization of uracil induced by proton and electron impact has been reported within the 20–150 keV and 8–16 eV ranges, respectively [30]. No cross section data for electron impact ionization were published, but it was shown that the most abundant species are the parent ion $C_4H_4N_2O_2^+$ and two fragment ions $C_3H_3NO^+$ and CNO^+. More recently, total cross sections for electron impact ionization of cytosine, thymine, adenine, and guanine have been calculated by Bernhard and Paretzke [29] with the Deutsch-Mark (DM) and BEB formalisms for energies ranging from the ionization threshold to 1000 eV. They observed that both algorithms yield very similar total electron impact ionization cross sections; only for higher impact energies is there a smaller decrease of the cross section with energy in the case of the BEB theory. In Fig. 6, the present ionization cross sections are compared with those obtained by Bernhardt and Paretzke [29] with the DM formalism. Qualitative behavior of both

Table 5 Total cross section for electron impact ionization of guanine, adenine, thymine, cytosine and uracil at selected energies

Energy (eV)	Ionization cross section (10^{-20} m^2)				
	Guanine	Adenine	Thymine	Cytosine	Uracil
10	0.575	0.545	0.171	0.457	0.0739
11	1.238	1.177	0.487	0.965	0.334
12	2.032	1.902	0.883	1.483	0.677
13	2.803	2.670	1.319	2.036	1.047
14	3.579	3.435	1.844	2.623	1.456
15	4.402	4.223	2.454	3.232	1.931
16	5.268	5.050	3.145	3.911	2.445
17	6.145	5.898	3.873	4.576	3.009
18	7.007	6.738	4.604	5.232	3.582
19	7.834	7.539	5.310	5.851	4.146
20	8.610	8.290	5.979	6.433	4.682
25	12.02	11.54	8.897	9.059	7.042
30	14.70	14.04	11.20	11.11	8.943
35	16.70	15.91	12.95	12.65	10.40
40	18.23	17.33	14.29	13.83	11.53
45	19.38	18.37	15.30	14.71	12.41
50	20.23	19.13	16.06	15.36	13.07
55	20.84	19.67	16.61	15.83	13.56
60	21.27	20.03	17.01	16.15	13.93
65	21.55	20.27	17.28	16.37	14.19
70	21.73	20.40	17.46	16.50	14.36
75	21.81	20.46	17.57	16.57	14.48
80	21.84	20.45	17.61	16.58	14.54
85	21.80	20.40	17.61	16.56	14.57
90	21.73	20.31	17.57	16.50	14.56
95	21.62	20.19	17.51	16.42	14.52
100	21.49	20.05	17.41	16.31	14.46
110	21.16	19.71	17.18	16.06	14.30
125	20.59	19.14	16.75	15.62	13.98
150	19.54	18.12	15.94	14.83	13.36
175	18.50	17.12	15.12	14.03	12.71
200	17.52	16.18	14.34	13.29	12.08
250	15.79	14.54	12.95	11.97	10.94
300	14.35	13.19	11.78	10.87	9.980
350	13.14	12.07	10.80	9.957	9.169
400	12.13	11.12	9.979	9.187	8.481
450	11.27	10.32	9.275	8.532	7.891
500	10.52	9.634	8.667	7.968	7.381
600	9.308	8.513	7.674	7.047	6.544
700	8.358	7.639	6.895	6.327	5.886
800	7.594	6.936	6.268	5.748	5.355
900	6.966	6.359	5.751	5.272	4.917
1000	6.439	5.876	5.318	4.873	4.549
1500	4.710	4.293	3.895	3.563	3.337
2000	3.743	3.409	3.097	2.831	2.656
2500	3.121	2.841	2.583	2.360	2.216
3000	2.684	2.443	2.222	2.030	1.907
3500	2.360	2.148	1.954	1.785	1.678
4000	2.110	1.919	1.747	1.595	1.500
4500	1.910	1.737	1.582	1.444	1.358
5000	1.746	1.588	1.446	1.320	1.242

data sets is almost the same, although some discrepancies exist mainly in the magnitude of the cross section (up to 10%) and threshold energies. Since in both calculations the same structural codes (GAUSSIAN and GAMESS) have been used, we can assume that the computational uncertainties in both ionization cross sections are very similar and therefore the observed discrepancies cannot be due to them. They can be correlated to the different computational approaches and especially to the *ab initio*

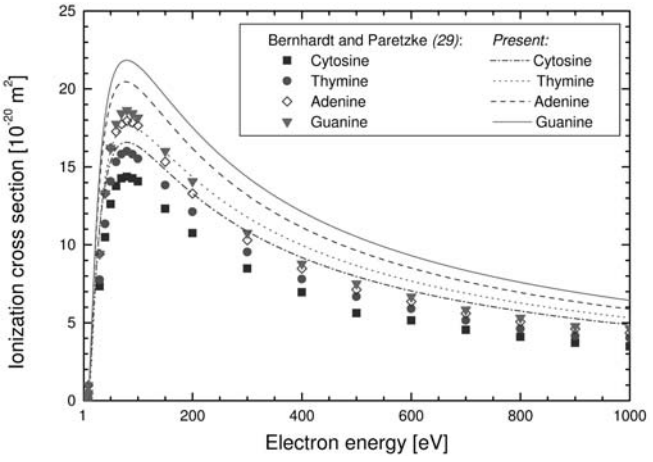

Fig. 6 Comparison between the present cross sections for ionization of the DNA bases calculated with the BEB model and the ionization cross sections for the same molecules obtained with the DM formalism by Bernhardt and Paretzke [29]

calculation of the binding energy of the first ionization potentials and the highest occupied molecular orbitals (HOMO). In the present work, the first ionization potentials (here it is assumed, according to the Koopman theorem that the calculated electron binding energy of the HOMO is the first ionization potential) were taken from experimental data [70, 71], which are in very close agreement with the values obtained theoretically [68] from the density functional theory (see Table 1). They are slightly lower (by about 0.3 eV for cytosine and thymine, 0.2 eV for adenine and 0.5 eV for guanine) than those of Bernhardt and Paretzke [29]. Moreover, in their calculations Bernhardt and Paretzke [29] took the binding energies of the HOMO generated at the Hartee-Fock level without any energy correlation of the electrons. These energies are about 1 eV higher than those used in the present work and may therefore account for differences between the two sets of data. It is worth noting that ionization potentials are lower in solution. For example calculations of the threshold of ionization for uracil and thymine molecules in water solution give values of 7.02 eV and 6.74 eV, respectively [78]. This means that according to the BEB formalism employed in the present work, the cross sections for electron impact ionization of DNA and RNA bases in water will be higher than in the gas phase. In such calculations the binding energies of higher occupied orbitals for DNA and RNA bases in the water solution should be taken into account but these are not presently available.

In summary, using simple computational models, the cross sections for elastic electron scattering and electron impact ionization of uracil, cytosine, thymine, adenine and guanine have been calculated at low and intermediate collision energies. It was found that the magnitude of the differential as well as integral elastic cross sections essentially depends on the number of electrons in the target and the molecular size. Similarly, the ionization cross sections strongly depend on the molecular size for energies ranging from 70 eV to 5000 eV. The results obtained can be useful for comparison with experimental results and in further studies of electron collisions with more complicated DNA and RNA components as well as with DNA and RNA. Such cross sections are also needed to describe in more details ionizing radiation damage to DNA and RNA via Monte Carlo simulations.

Acknowledgments This work was supported by the Canadian Institutes of Health Research.

Appendix A

The Schrödinger Eq. 3 is a differential equation of the following form:

$$\frac{d^2}{dr^2}u_l(r) = F_l(r)u_l(r) \tag{12}$$

where:

$$F_l(r) = -2\left(E - V(r) - \frac{l(l+1)}{2r^2}\right) \tag{13}$$

In our caclulations, we integrated Eq. 12 using the Numerov method [51], in which:

$$\left[1 - \frac{1}{12}(\Delta r)^2 F_l(r_{j+1})\right]u_l(r_{j+1}) - 2\left[1 + \frac{5}{6}(\Delta r)^2 F_l(r_j)\right]u_l(r_j) + \left[1 - \frac{1}{12}(\Delta r)^2 F_l(r_{j-1})\right]u_l(r_{j-1}) = 0 \tag{14}$$

where Δr is the increment in the method and in the presented calculations Δr=0.01.

Appendix B

The Bessel-Riccati and Neumann-Riccati functions [52] obey the following relationships:

$$\frac{d}{dx}\hat{z}_l(x) + \frac{l}{x}\hat{z}_l(x) - \hat{z}_{l-1}(x) = 0 \tag{15}$$

and

$$\frac{d}{dx}\hat{z}_l(x) - \left(\frac{l+1}{x}\right)\hat{z}_l(x) + \hat{z}_{l+1}(x) = 0 \tag{16}$$

where $x=kr$, and $\hat{z}_l(x)$ represents Bessel-Riccati, $\hat{j}_l(x)$, and Neumann-Riccati, $\hat{n}_l(x)$, functions, respectively. It follows from Eqs. 15 and 16 that:

$$\hat{z}_{l+1}(x) = \frac{2l+1}{x}\hat{z}_l(x) - \hat{z}_{l-1}(x) \tag{17}$$

Using Eq. 17 it is possible to generate any Bessel-Riccati and Neuman-Riccati function for $l \geq 2$.

For $l=0$ and $l=1$, the Bessel-Riccati and Neumann-Riccati functions have the following form:

$$\hat{j}_0(x) = \sin x \tag{18}$$

$$\hat{j}_1(x) = -\cos x + \frac{\sin x}{x} \tag{19}$$

$$\hat{n}_0(x) = -\cos x \tag{20}$$

and

$$\hat{n}_1(x) = -\sin x - \frac{\cos x}{x} \tag{21}$$

Since in the present calculations, the argument x=kr can reach large values, we generated Bessel-Riccati and Neumann-Riccati functions from the following relationships:

$$\hat{j}_l(x) = \left[P\left(l+\frac{1}{2},x\right)\sin\left(x-\frac{1}{2}l\pi\right) + Q\left(l+\frac{1}{2},x\right)\cos\left(x-\frac{1}{2}l\pi\right)\right] \tag{22}$$

and

$$\hat{n}_l(x) = (-1)^{l+1}\left[P\left(l+\frac{1}{2},x\right)\cos\left(x+\frac{1}{2}l\pi\right) - Q\left(l+\frac{1}{2},x\right)\sin\left(x+\frac{1}{2}l\pi\right)\right] \tag{23}$$

where

$$P\left(l+\frac{1}{2},x\right) = \sum_{i=0}^{[l/2]}(-1)^i\left(l+\frac{1}{2},2i\right)(2x)^{-2i} \tag{24}$$

and

$$Q\left(l+\frac{1}{2},x\right) = \sum_{i=0}^{[(l-1)/2]}(-1)^i\left(l+\frac{1}{2},2i+1\right)(2x)^{-2i-1} \tag{25}$$

In the above equations

$$\left(l+\frac{1}{2},i\right) = \frac{(l+i)!}{l!\Gamma(l-i+1)} \tag{26}$$

References

1. Hoppe W, Lohmann W, Markl H, Ziegler H (eds) (1983) Biophysics. Springer, Berlin
2. Goodhead DT (1994) Initial events in the cellular effects of ionizing radiations: clustered damage in DNA. Int J Radiat Biol 65:7–17
3. Symons MCR (1994) Direct and indirect damage to DNA by ionizing radiation. Radiat Phys Chem 43:403–405
4. Ward JF, Webb CF, Limoli CL, Milligan JR (1990) DNA lesions produced by ionizing radiation locally multiply damaged sites. In: Wallace SS, Painter RB (eds) Ionizing radiation damage to DNA: molecular aspects. Wiley-Liss, New York, pp 43–50
5. Pomplun E, Terrissol M, Demonchy M (1996) Modelling of initial events and chemical behaviour of species induced in DNA units by auger electrons from ^{125}I, ^{123}I and carbon. Acta Oncol 35:857–862
6. Nikjoo H, O'Neill P, Goodhead DT, Terrissol M (1997) Computational modelling of low-energy electron-induced DNA damage by early physical and chemical events. Int J Radiat Biol 71:467–483
7. Moiseenko VV, Hamm RN, Walker AJ, Prestwich WV (1998) Modelling DNA damage induced by different energy photons and tritium beta-particles. Int J Radiat Biol 74:533–550
8. Nikjoo H, O'Neill P, Terrissol M, Goodhead DT (1999) Quantitative modelling of DNA damage using Monte Carlo track structure method. Radiat Environ Biophys 38:31–38
9. Uehara S, Nikjoo H, Goodhead DT (1999) Comparison and assessment of electron cross sections for Monte Carlo track structure codes. Radiat Res 152:202–213
10. Bernhardt P, Friedland W, Jacob P, Paretzke HG (2003) Modeling of ultrasoft X-ray induced DNA damage using structured higher order DNA targets. Int J Mass Spectrom 223/224:579–597
11. Terrissol M, Beaudré A (1990) Simulation of space and time evolution of radiolytic species induced by electrons in water. Radiat Prot Dosim 31:171–175
12. Ritchie RH, Hamm RN, Turner JE, Wright HA, Bloch WE (1991) Radiation interactions and energy transport in the condensed phase. In: Glass WA, Varma MN (eds) Physical and chemical mechanisms in molecular radiation biology. Plenum Press, New York, pp 99–135
13. Friedland W, Jacob P, Paretzke HG, Stork T (1998) Monte Carlo simulation of the production of short DNA fragments by low-linear energy transfer radiation using higher-order DNA models. Radiat Res 150:170–182
14. Friedland W, Jacob P, Paretzkee HG, Merzagora M, Ottolenghi A (1999) Simulation of DNA fragment distributions after irradiation with photons. Radiat Environ Biophys 38:39–47
15. Boudaiffa B, Cloutier P, Hunting D, Huels MA, Sanche L (2000) Resonant formation of DNA strand breaks by low-energy (3–20 eV) electrons. Science 287:1658–1660
16. Boudaiffa B, Cloutier P, Hunting D, Huels MA, Sanche L (2002) Cross section for low-energy (10–50 eV) electron damage to DNA. Radiat Res 157:227–234
17. Boudaiffa B, Hunting D, Cloutier P, Huels MA, Sanche L (2000) Induction of single- and double-strand breaks in plasmid DNA by 100–1500 eV electrons. Int J Radiat Biol 76:1209–1221
18. Folkard M, Prise KM, Vojnovic B, Davies S, Roper MJ, Michael BD (1993) Measurement of DNA damage by electrons with energies between 25 and 4000 eV. Int J Radiat Biol 64:651–658
19. Huels MA, Boudaiffa B, Cloutier P, Hunting D, Sanche L (2003) Single, double and multiple double strand breaks induced in DNA by 3–100 eV electrons. J Am Chem Soc 125:4467–4477
20. Sanche L (2002) Nanoscopic aspects of radiobiological damage: fragmentation induced by secondary electrons. Mass Spectrom Rev 21:349–369
21. ICRU (1979) Average energy required to produce an ion pair. Report 31, International Commission on Radiation Units and Measurements. Bethesda, MD
22. Cobut V, Fongillo Y, Patau JP, Goulet T, Fraser MJ, Jay-Gerin JP (1998) Monte-Carlo simulation of fast electron and proton tracks in liquid water.I. Physical and physico-chemical aspects. Radiat Phys Chem 51:229–243
23. Abdoul-Carime H, Cloutier P, Sanche L (2001) Low-energy (5–40 eV) electron-stimulated desorption of anions from physisorbed DNA bases. Radiat Res 155:625–633
24. Herve du Penhoat M-A, Huels MA, Cloutier P, Jay-Gerin J-P, Sanche L (2001) Electron stimulated desorption of H^- from thin films of thymine and uracil. J Chem Phys 114:5755–5764
25. Barrios R, Skurski P, Simons J (2002) Mechanism for damage to DNA by low-energy electrons. J Phys Chem B 106:7991–7994
26. Huels MA, Hahndorf I, Illenberger E, Sanche L (1998) Resonant dissociation of DNA bases by subionization electrons. J Chem Phys 108:1309–1312

27. Pan X, Cloutier P, Hunting D, Sanche L (2003) Dissociative electron attachment to DNA. Phys Rev Lett 90:208102/1–208102/4
28. Lévesque PL, Michaud M, Sanche L (2003) Cross section for low energy (1–12 eV) inelastic electron scattering from condensed thymine. Nucl Instr Methods Phys Res B (in press)
29. Bernhardt Ph, Paretzke HG (2003) Calculation of electron impact ionization cross sections of DNA using the Deutsch-Mark and Binary-Encounter-Bethe formalisms. Int J Mass Spectrom 223/224:599–611
30. Coupier B, Farizon B, Farizon M et al. (2002) Inelastic interactions of protons and electrons with biologically relevant molecules. Eur Phys J D 20:459–468
31. Mott NF, Massey HSW (1965) The theory of atomic collisions. Oxford University Press, Oxford
32. Raj D (1991) A note on the use of the additivity rule for electron-molecule elastic scattering. Phys Lett A 160:571–574
33. Możejko P, Żywicka-Możejko B, Szmytkowski Cz (2002) Elastic cross section calculations for electron collisions with XY_4 (X=Si,Ge; Y=H,F,Cl,Br,I) molecules. Nucl Instr Methods Phys Res B 196:245–252
34. Jiang Y, Sun J, Wan L (2000) Additivity rule for the calculation of electron scattering from polyatomic molecules. Phys Rev A 62:712
35. Khare SP, Raj D, Sinha P (1994) Absorption effects in the elastic scattering of electrons by the CF_4 molecules at intermediate energies. J Phys B 27:2569–2579
36. Sun J, Jiang Y, Wan L (1994) Total cross sections for electron scattering by molecules. Phys Lett A 195:81–83
37. Jiang Y, Sun J, Wan L (1995) Total cross sections for electron scattering by polyatomic molecules at 10–1000 eV: H_2S, SiH_4, CH_4, CF_4, CCl_4, SF_6, C_2H_4, CCl_3F, $CClF_3$ and CCl_2F_2. Phys Rev A 52:398–403
38. Joshipura KN, Vinodkumar M (1997) Total cross sections of electron collisions with S atoms; H_2S, OCS and SO_2 molecules ($E_i \geq 50$ eV). Z Phys D 41:133–137
39. Liu Y, Sun J, Li Z, Jiang Y, Wan L (1997) Total cross sections for electron scattering from molecules: NH_3 and H_2O. Z Phys D 42:45–48
40. Raj D, Tomar S (1997) Electron scattering by triatomics: SO_2, CS_2 and OCS at intermediate energies. J Phys B 30:1989–1999
41. Raizada R, Baluja KL (1997) Total cross sections of positron scattering from various molecules using the rule of additivity. Phys Rev A 55:1533–1536
42. Maji S, Basavaraju G, Bharathi SM, Bhushan KG, Khare SP (1998) Elastic scattering of electrons by polyatomic molecules in the energy range 300–1300 eV: CO, CO_2, CH_4, C_2H_4 and C_2H_6. J Phys B 31:4975–4990
43. Joshipura KN, Vindokumar M (1999) Various total cross-sections for electron impact on C_2H_2, C_2H_4 and CH_3X (X=CH_3; OH; F; NH_2). Eur Phys J D 5:229–235
44. Reid DD, Wadhera JM (1999) Scattering of intermediate-energy positrons by C, N, O atoms and the corresponding diatomic molecules: elastic and total cross-sections. Chem Phys Lett 311:385–389
45. Pablos JL de, Kendall PA, Tegeder P, Williart A, Blanco F, Garcia G, Mason N (2002) Total and elastic electron scattering cross sections from ozone at intermediate and high energies. J Phys B At Mol Opt Phys 35:865–874
46. Schmidt MW, Baldridge KK, Boatz JA et al. (1993) General atomic and molecular electronic structure system. J Comp Chem 14:1347–1363
47. Krishnan R, Binkley JS, Seeger R, Pople JA (1980) Self-consistent molecular orbital methods. XX. A basis set for correlated wave functions. J Chem Phys 72:650–654
48. Haromy PT, Hunter WN, Kennard O, Saenger W, Sundaralingam M (1989) Crystallographic and structural data I. Springer, Berlin
49. Dolgounitcheva O, Zakrzewski VG, Ortiz JV (2002) Ionization energies and Dyson orbitals of thymine and other methylated uracils. J Phys Chem A 106:8411–8416
50. Rodberg LS, Thaler RM (1967) Introduction to the quantum theory of scattering. Academic Press, New York
51. Hartree DR (1957) The calculation of atomic structures. John Wiley, New York
52. Abramowitz M, Stegun IA (1970) Handbook of mathematical functions. Dover Publications, New York
53. Salvat F, Martinez JD, Mayol R, Parellada J (1987) Analytical Dirac-Hartree-Fock-Slater screening function for atoms (Z=1–92). Phys Rev A 36:467–474
54. Padial NT, Norcross DW (1984) Parameter-free model of the correlation-polarization potential for electron-molecule collisions. Phys Rev A 29:1742–1748
55. Pedrew JP, Zunger A (1981) Self-interaction correction to density-functional approximations for many-electron systems. Phys Rev B 23:5048–5079
56. Zhang X, Sun J, Liu Y (1992) A new approach to the correlation polarization potential—low-energy electron elastic scattering by He atoms. J Phys B 25:1893–1897
57. Szmytkowski Cz, Szmytkowski R (1994) On the contribution of higher partial waves to scattering by the long-range inverse power potentials. Z Nauk PG Fizyka 30:19–25
58. Możejko P, Żywicka-Możejko B, Szmytkowski Cz (2000) Elastic cross section calculations for electron scattering on polyatomic molecular targets: XY_4 (X=C, Si, Ge; Y=H, F, Cl), XF_6 (X=S, W, U), C_2F_6 and C_6Y_6 (Y=H, F). Uzhhorod University Science Herald Physics 8:108–111
59. Kim YK, Rudd ME (1994) Binary-encounter-dipole model for electron-impact ionization. Phys Rev A 50:3954–3967
60. Hwang W, Kim YK, Rudd ME (1996) New model for electron-impact ionization cross sections of molecules. J Chem Phys 104:2956–2966
61. Mott NF (1930) The collision between two electrons. Proc R Soc Lond A 126:259
62. Bethe H (1930) Zur Theorie des Durchgangs schneller Korpuskularstrahlen durch Materie. Ann Phys (Leipzig) 5:325–400
63. Bethe H (1932) Bremsformel für Elektronen relativistischer Geschwindigkeit. Z Phys 76:293–299
64. Kim YK, Hwang W, Weinberger NM, Ali MA, Rudd ME (1997) Electron-impact ionization cross sections of atmospheric molecules. J Chem Phys 106:1026–1033
65. Ali MA, Kim YK, Hwang W, Weinberger NM, Rudd ME (1997) Electron-impact total ionization cross sections of silicon and germanium hydrides. J Chem Phys 106:9602–9608
66. Nishimura H, Huo WM, Ali MA, Kim YK (1999) Electron-impact total ionization cross section of CF_4, C_2F_6 and C_3F_8. J Chem Phys 110:3811–3822
67. Russo N, Toscano M, Grand A (2002) Theoretical determination of electron affinity and ionization potential of DNA and RNA bases. J Comp Chem 21:1243–1250
68. Wetmore SD, Boyd RJ, Eriksson LA (2000) Electron affinities and ionization potentials of nucleotide bases. Chem Phys Lett 322:129–135
69. Sevilla MD, Becker D, Yan M, Sommerfield SR (1991) Relative abundances of primary ion radicals in γ-irradiated DNA: cytosine vs thymine and guanine vs adenine cations. J Phys Chem 95:3409–3415
70. Orlov VM, Smirnov AM, Varshavsky YM (1976) Ionization potentials and electron-donor ability of nucleic acid bases and their analogues. Tetrahedron Lett 48:4377–4378
71. Verkin BI, Sukhodub LF, Yanson IK (1976) Ionization potentials of nitrogenous bases of nucleic acids. Dokl Biophys 226–228:100–103
72. Hwang CT, Stumpf CL, Yu Y-Q, Kenttämaa HI (1999) Intrinsic acidity and redox properties of the adenine radical cation. Int J Mass Spectrom 182/183:253–259
73. Cederbaum LS (1975) One-body Green's function for atoms and molecules: theory and application. J Phys B 8:290–303
74. Niessen W von, Schirmer J, Cederbaum LS (1984) Computational methods for the one-particle Green's function. Comp Phys Rep 1:57–125

75. Ortiz JV (1988) Electron binding energies of anionic alkali metal atoms from partial fourth order electron propagator theory calculations. J Chem Phys 89:6348–6352
76. Zakrzewski VG, Niessen W von (1994) Vectorizable algorithm for Green function and many-body perturbation methods. J Comp Chem 14:13–18
77. Frisch MJ, Trucks GW, Schlegel HB et al. (2001) Gaussian 98, evision A.11.2. Gaussian Inc., Pittsburgh PA
78. Wetmore SD, Boyd RJ, Eriksson LA (2001) A theoretical study of 5-halouracils: electron affinities, ionization potentials and dissociation of the related anions. Chem. Phys Lett 343:151–158